Investigation of a high Reynolds number turbulent boundary layer flow with adverse pressure gradients using PIV and 2D- and 3D- Shake-The-Box

A. Schröder[1], D.Schanz[1], M.Novara[1], F. Philipp[1], R. Geisler[1], J. Agocs[1], T. Knopp[1], M. Schroll[2] and C. E. Willert[2]

1: German Aerospace Center (DLR), Institute of Aerodynamics and Flow Technology, Göttingen, Germany
2: German Aerospace Center (DLR), Institute of Propulsion Technology, Cologne, Germany
* Correspondent author: andreas.schroeder@dlr.de

Keywords: Shake-The-Box, PIV, turbulent boundary layer, adverse pressure gradient

ABSTRACT

We present an experimental adverse pressure gradient turbulent boundary layer (TBL) flow investigation at high Reynolds numbers (approx. 10.000 < Re_θ < 40.000) using large field multi-camera 2D PIV and three different particle tracking methods based on the Shake-The-Box (STB) technique, namely time-resolved 2D- and 3D-STB and Multi-Pulse (MP-) STB. The experiments were performed within the frame of the DLR project *Victoria* and conducted in the Eiffel type atmospheric wind tunnel of the University of Armed Forces in Munich (AWM), which has a 22-m-long test section with a rectangular cross section of 1.8 × 1.8 m^2. After a ramp the TBL develops along a flat plate with nearly zero pressure gradients (ZPG) to an equilibrium state before it enters into a 2D diffusor geometry following a smooth and moderate curvature into a flat plate at ~18° inclination angle while undergoing a significant adverse pressure gradient (APG) leading to flow separation. The measurements have been performed with an embedded field-of-view (FOV) strategy. A statistical significant number of samples for four different free stream velocities have been acquired at several positions in all pressure gradient regimes down to the region of (intermittent) flow separation. A large number of instantaneous velocity vector fields and time-resolved particle tracks of the boundary layer flow have been achieved in order to gain high resolution wall-normal profiles of the mean velocities and related Reynolds stresses $<u'_iu'_j>$ in a first step.

1. Introduction

The characterization of adverse pressure gradient turbulent boundary layer (APG-TBL) flows at high Reynolds numbers is an important open topic of research due to its technical importance e.g. for high-lift wing configurations or flows around bluff bodies. This is not only true for the research of unsteady dynamics of multiple scales involved in the spatial and temporal development of coherent structures and related wall-shear stress events. Even when looking at the development of mean velocity (and Reynolds stress) statistics the overall behavior of the flow is not yet described properly in a universal manner neither along the wall nor across the full boundary layer thicknesses (Knopp et al. 2014 and 2015). Related data gained experimentally and numerically are available in the literature and existing attempts to find proper (semi-) empirical scaling laws for the velocity profiles show (partial) validity for several limited regions at certain wall-normal distances e.g. (Nickels 2004) (Maciel et al. 2006). Nevertheless, some data still show significant discrepancies to the existing scaling laws in the respective wall-normal regions e.g. due to a lack of measurement accuracy and/or due to history effects of the underlying multi-scale flow dynamics of the chosen specific flow geometry. In order to find a more universal description in such flows with scaling laws across the whole δ (most likely in a composite way) new experimental data are necessary which fulfill the requirements of resolving all relevant turbulent flow properties at high accuracies, especially close to the wall e.g. for determining directly the wall-shear-stress τ_w. Therefore, for TBL flows at high and industrially relevant Reynolds numbers ($Re_\theta > 10{,}000$) appropriate measurement techniques still need to be adapted and developed that are able to deliver unsteady (or even time-resolved) three-component velocity information at high spatial resolution preferably in a whole volume of the flow at many points simultaneously. At moderate Reynolds numbers PIV and STB are proven methods for delivering accurate velocity data in turbulent flows within relatively short measurement times as well suited for statistical means. While PIV is only useful for regions with moderate velocity gradients (in our case in the outer flow region of the TBL), STB, or high magnification particle tracking approaches, are suited to deliver the required velocity data in close vicinity to walls or in strong shear-layers (more generally in areas where strong mean and instantaneous velocity gradients are dominant). MP-STB is matured now to bridge the gap between both methods due to the availability of high-laser pulse energy and high resolution cameras (see Novara et al. 2016 and Novara et al. 2018); furthermore it allows measurements in high-speed flows (Manovski et al. 2016). Based on the available large numbers of individual particle trajectories from 2D- and 3D-STB evaluations, and after applying a proper temporal filtering with optimal B-Splines (Gesemann et al. 2016), the gained results can be used for bin-averaging approaches delivering highly resolved (subpixel resolution) profiles of mean velocity components, Reynolds stresses (Schröder et al. 2015a/b) and triple-correlation terms. Furthermore, two-point statistics of particles velocities and accelerations or Navier-Stokes regularized data assimilation and interpolation methods, like FlowFit (Gesemann et al. 2016) or VIC+ (Schneiders et al. 2016), can be used to deduce the instantaneous velocity gradient tensor, local energy dissipation rate ε, spectra etc.

2. Experimental set-up and procedure

We performed the present APG-TBL experiment in the Eiffel type atmospheric wind tunnel of UniBw in Munich, which has a 22-m-long test section with a rectangular cross section of 1.8 × 1.8 m^2 and sufficient optical access for all used particle based measurement systems. As shown in Fig. 1 the flow develops on the wind tunnel wall over a few meters and is then accelerated in a FPG region along a first ramp with smooth curvatures of height 0.44 m and of length 1.20 m. Then the flow relaxes along a flat plate of length 4.0 m at nearly ZPG towards equilibrium. The TBL flow then follows two slight curvilinear deflections over a length of 1.17 m which initially causes a small FPG, and enters into the APG region of a subsequent flat plate with an inclination angle of approximately 18° and length of 763 mm (projection to x-axis). Finally, the flow separates for all measured velocities along that plate which intersects with the wind tunnel wall at the position of the defined origin of the coordinate system (see Fig. 1 bottom) with x-axis in flow direction, y-axis wall-normal and z-axis spanwise and z = 0 in the centerline of the wind tunnel wall.

The experiments were performed at four different boundary layer edge velocities U_e = 21.07 m/s, U_e = 26.61m/s, U_e = 29.25 m/s, and U_e = 35.48 m/s. The wind tunnel velocity was proven to be stable with less than 0.08 m/s standard deviation for all U_e using an online PIV measurement system which was operated in parallel for all flow cases at a reference position above the boundary layer edge in the ZPG region at x = -2600 mm. The development of the pressure coefficients c_p for U_e = 35.48 m/s is shown in the graph at Fig. 1-top, indicating smooth pressure gradients along the wall in flow direction for two flow parallel pressure tap rows shifted along the spanwise direction (z = ± 550 mm). Further pressure tap rows, placed at other spanwise positions in the APG region at the flat plate with ~18° inclination angle, show a sufficient 2D behavior of the mean flow even close to the mean flow separation region.

DEHS particles with a mean diameter of ~~ 1μm were generated by Laskin type nozzles and introduced into the Eiffel type wind tunnel at two positions simultaneously: Particles were guided through a small chamber and a spanwise slit in the wind tunnel wall, immediately downstream of the honeycombs and meshes and upstream of the turbulent boundary layer flow (s.c. wall seeding). Additionally, particles were introduced with a mesh of perforated tubes at the intake of the wind tunnel on the top of the halls ceiling (s.c. free-stream seeding) enabling a homogenous distribution with adaptable seeding densities within the measurement volumes.

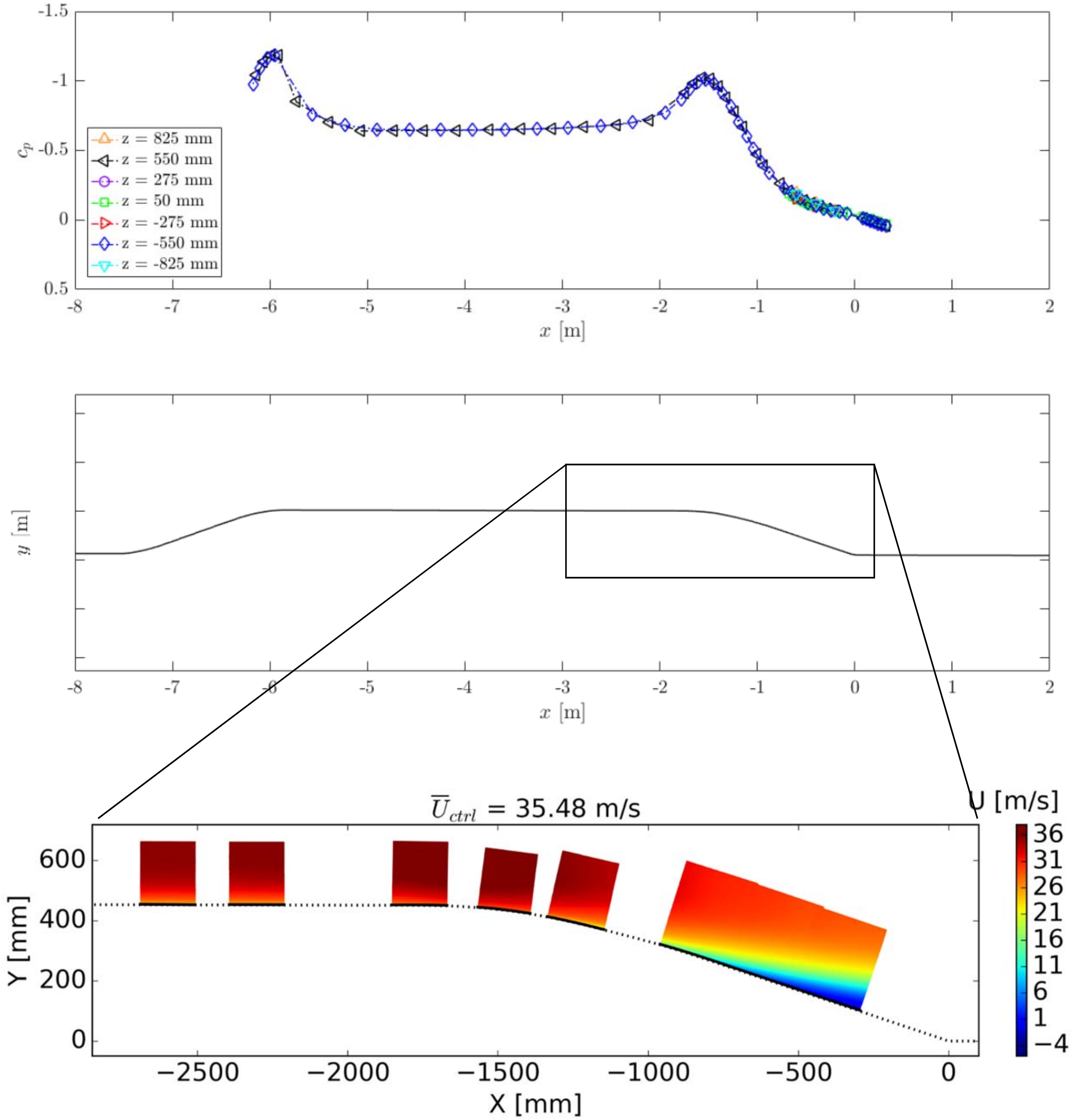

Figure 1: *Top:* c_p distribution of the TBL development along the present wall model of the *DLR Victoria* project with the following succession of pressure gradient regimes in flow direction: FPG, ZPG, FPG and finally APG. *Middle:* Contour of the wall model with defined coordinate system origin at the downstream intersection of the APG model part with the wind tunnel wall. *Bottom:* Mean u-velocity contour field results for the case of U_e = 35.48 m/s based on the overview PIV measurements using 8 sCMOS cameras.

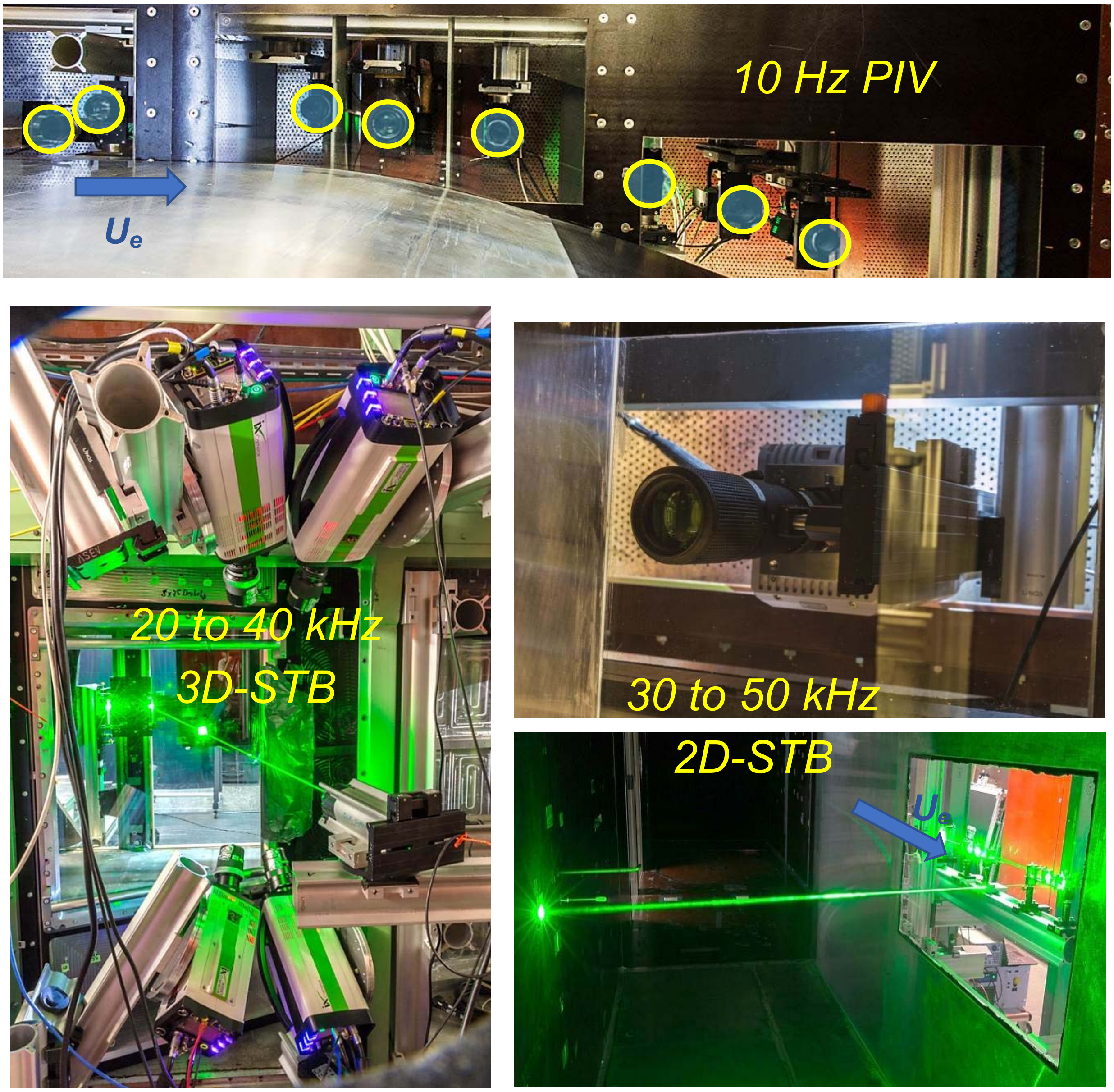

Figure 2: *Top:* Overview PIV configuration using 8 x sCMOS cameras from PCO (5.6 Mpx each) aligned with partly overlapping FOVs along the wall contour of the TBL. *Left-bottom:* Pyramidal camera set-up in forward scattering modus for high-repetition rate 3D-STB operating up to 40,000 kHz; four new *IX iSpeed726* cameras viewing through the glass window onto a wall normal light volume column were employed. *Right-middle and bottom: Photron SA-X2* viewing perpendicular onto a thin light-sheet column for 2D-STB measurements of the velocity profile up to 50,000 kHz.

The overview measurements were performed with eight partly overlapping sCMOS cameras from *PCO* with 5.6 Mpx resolution each. The fields of view of the eight PIV cameras are shown in Fig. 1 bottom; the cameras placed on the top of the wind tunnel test section with Zeiss f = 100 mm and f = 80 mm lenses are shown in Fig. 2 top. Laser illumination was realized with two overlapping double-pulsed Nd:YAG Evergreen 200 lasers with ~400 mJ each and a light sheet introduced from an upstream position through a small window in the opposite wind tunnel wall allowing for a tangential illumination of the APG wall.

The 2D-STB system was operated with a Photron SA-X2 high speed camera with 20 μm pixel sizes equipped with a f = 200 mm Nikon lens with a 2x-teleconverter (see Fig. 2 right-middle) in a reduced resolution modus of 152 x 1024 pixels, corresponding to 6.6 x 45 mm² FOV, in x- and y-direction and a frame rate between 25 - 50 kHz depending on the flow velocity. Illumination was provided in a focused beam of ~6 mm extension in x- or flow direction and ~800 μm thickness by a high repetition rate *blizz* laser from *Innolas* with 38 W total power at 30 to 50 kHz (see Fig. 2 right-bottom). In order to avoid pixel locking an optical diffuser filter from LaVision (Michaelis et al. 2016) was used in front of the sensor. For all four U_e velocities, three times 294,000 time-resolved images per run (divided in statistical independent chunks of 1024 images) have been acquired at ~23 px/mm (~43 μm/px) resolution at two streamwise locations of the TBL flow (see Fig. 4) in order to fulfill the requirements for statistical convergence.

The 3D-STB system used four *i-Speed726* CMOS cameras from *iXCameras* with 13.5 μm pixel size equipped with f = 100 mm Zeiss macro lenses and with teleconverter (2x magnification) in Scheimpflug mounts from LaVision. The cameras were operated in a pyramidal geometric set-up in similar forward scattering directions looking through the wind tunnel window glass with 13 mm thickness (see Fig. 2 left). As for the 2D-STB camera, pixel locking is avoided with optical diffuser filters from LaVision. The laser illumination was provided as well with the *blizz* laser from *Innolas*. The beam was introduced through a window from the opposite side of the test section, shaped and collimated by optics to an elliptical beam and cut by a pass-partout to a cross-section of ~9 x 2 mm² in flow and wall-normal directions. With a reduced resolution of 252 x 2048 pixels the *i-Speed726* cameras are able to acquire frames at 40 kHz. The common measurement volume has a size of 9 x 85 x 2 mm³ in mean flow, wall-normal and spanwise directions (see Fig. 3 left). Due to the angular viewing at high image magnifications high Scheimpflug angles have to be realized which, together with the astigmatism caused by the thick window glass, lead to optically distorted particle images. Therefore, the volume-self calibration procedure was complemented with a calibration of the optical transfer function (OTF) (Schanz et al. 2013) (see Fig. 3 right). A frame rate between 20 to 40 kHz was used for the image acquisition of three times 98,640 images per flow case in statistical independent chunks of 109 time-resolved images in order to reach convergence requirements. Nevertheless, the intermittent flow separation present for all velocities at the measurement position (see Fig. 4) generates very low speed flows in the FOV; as a consequence convergence of statistics can be reached here only by averaging over very long time sequences or with significantly lower frame rates.

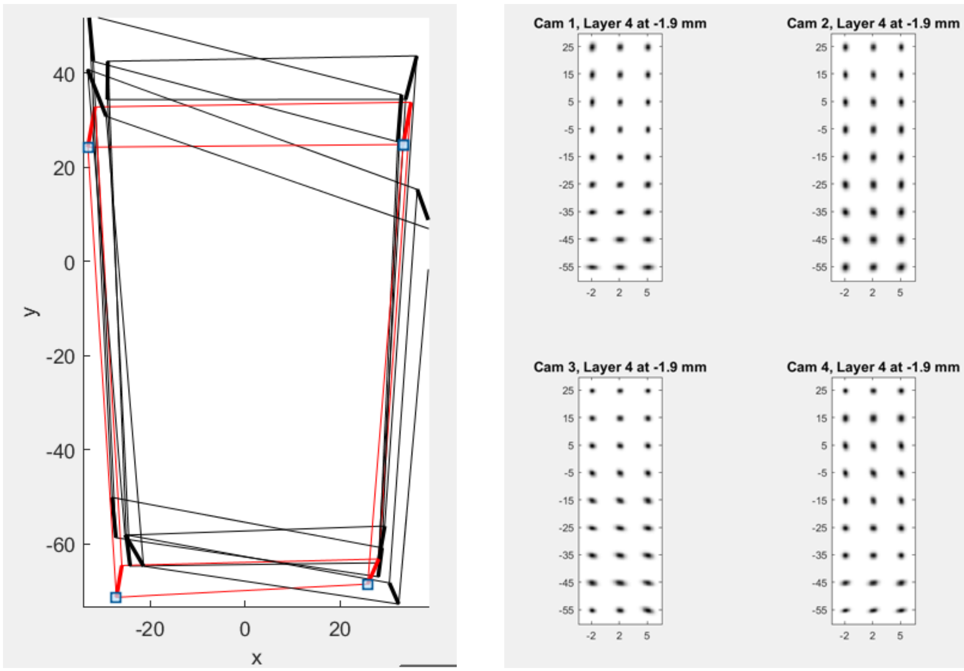

Figure 3: *Left:* Calibration result of common 3D-STB measurement volume at the wall in the APG region (9 x 85 x 2 mm³); *Right:* Result of the calibration of the particles optical transfer function (OTF) of all four cameras in one z-plane

For the Multi-Pulse STB system a novel strategy based on multi-exposed frames has been chosen: Four sCMOS cameras from PCO have been used in 90° light scattering modus to image a volume of 80 x 90 x 6 mm³ (wall-parallel, wall-normal and span-wise directions respectively) located in the APG region of the TBL flow (location shown by the red box in Fig. 4). Two *BigSky400* PIV laser systems, providing four pulses with 200 mJ each, have been used to obtain a collimated and pass-partout-cut particle illumination; the laser light was introduced almost perpendicular to the polished aluminum of the wind tunnel wall. In order to increase the dynamic velocity range, an uneven pulse separation strategy was adopted, where the time separation between pulses 2 - 3 was three times larger than the one between pulses 1 - 2 and 3 – 4; the time separation is adjusted according to the free stream velocity U_e (ranging from approximately 20 to 36 m/s). For details regarding the MP-STB the authors refer to Novara et al.

2018. The locations and FOV of all particle based methods involved in the present campaign, and the positions chosen for the extraction of wall-normal profiles are shown in Fig. 4.

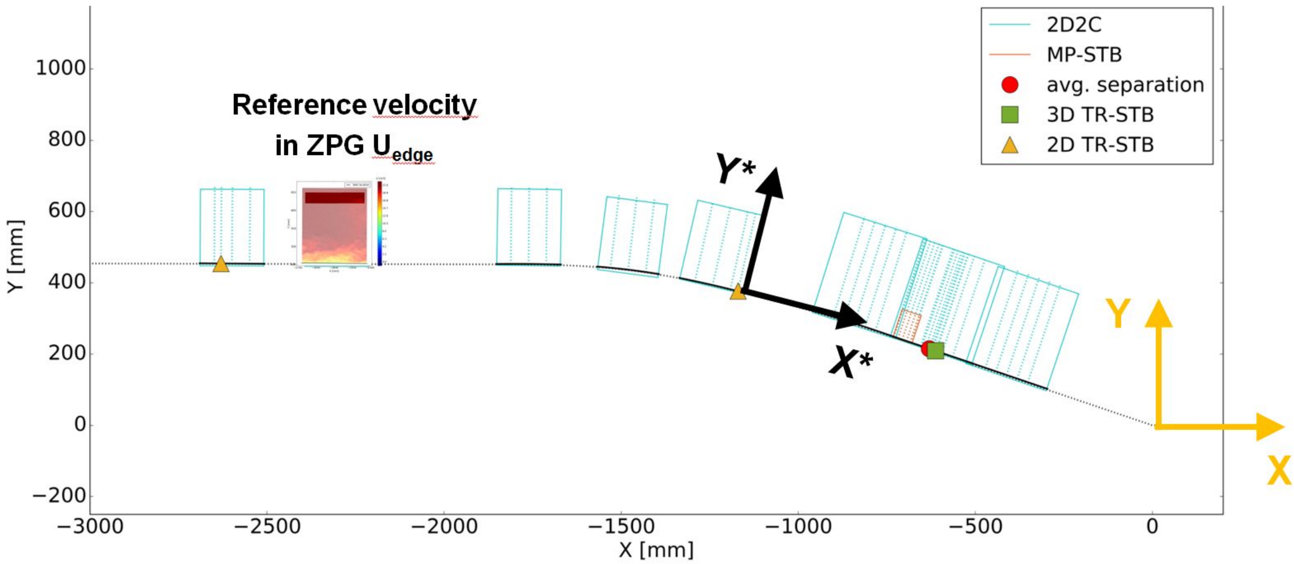

Figure 4: Locations of the measurement volumes for the particle based velocimetry and tracking methods applied in the present investigation (only the mid-point of the FOV along the wall-parallel direction is shown for the 2D and 3D time-resolved STB measurements). The second downstream PIV camera was operated in parallel to each measurement for online control of U_e

3. Evaluation and results

The evaluation of the 2D-PIV overview measurements with 8 cameras and 16,000 snapshot samples per flow case was performed, after proper image preprocessing, with an iterative multi-grid 2D cross-correlation approach with window deformation in *PIVview3.70* from *PivTec* starting with an initial window size of 128 x 128 px² and ending with a final window size of 24 x 14 px², corresponding to ~ 1.2 x 2 mm² in the ZPG area (f = 100 mm lenses) and approx. 1.6 x 2.7 mm² in the APG area (f = 80 mm lenses), in flow and wall-normal direction. A rectangular correlation window was chosen in order to enhance the spatial resolution for the resulting wall-normal velocity profiles, while the vector pitch was aligned at 66% overlap in both directions. Finally universal outlier detection (Scarano and Westerweel 2005) and a coordinate transformation into the common wind tunnel model system have been applied. The wall position was found on the camera images aided by an intial guess from the average image (i.e. average wall location). The time-history of the instantaneous wall-surface location suggested vibrations up to ~0.3 px that, given the size of the cross-correlation window, can be considered negligible.

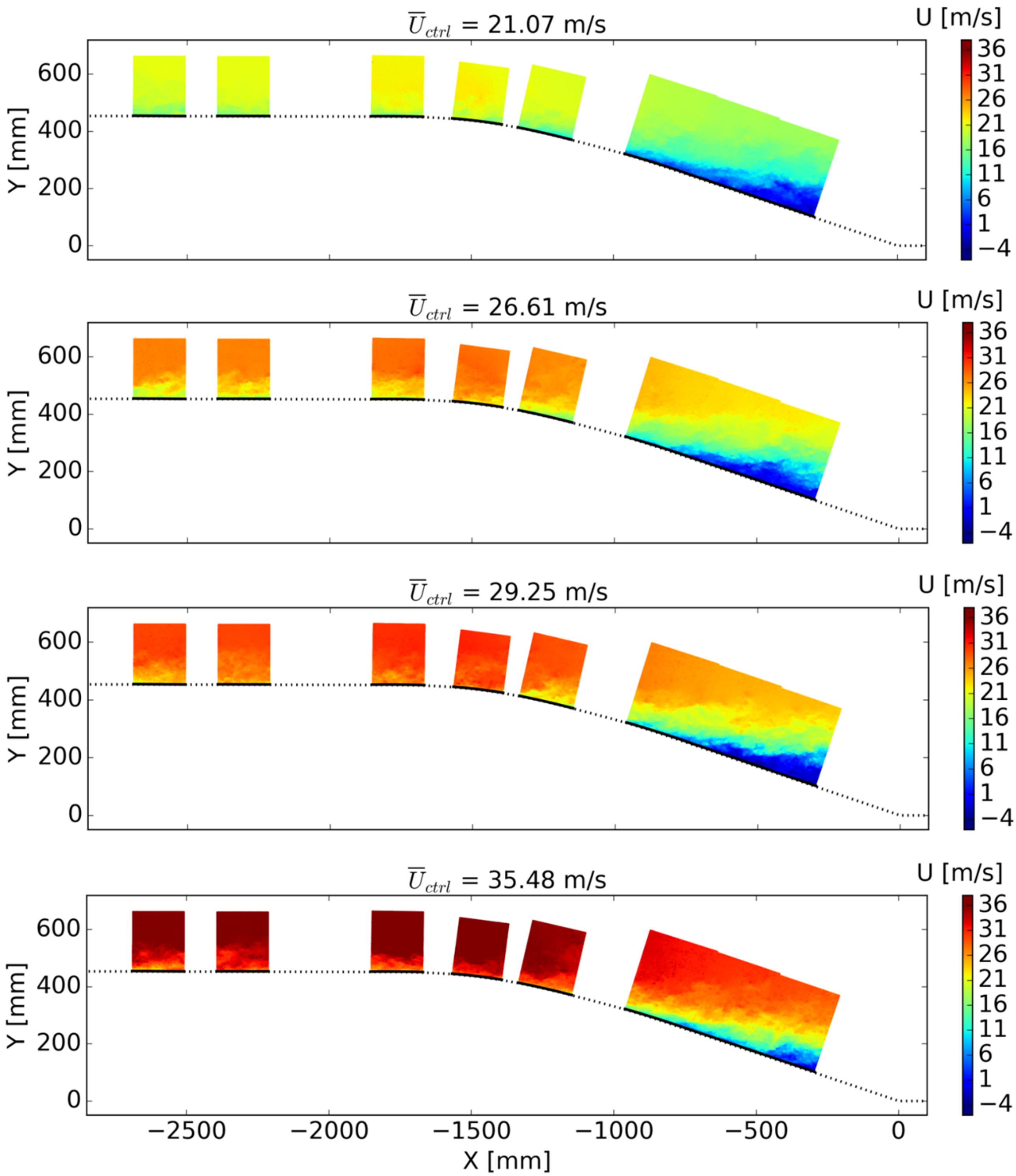

Figure 5: Instantaneous u-velocity distributions of the TBL flow along the wall contour evaluated by 2D-PIV (u-velocity contour color coded) for the four investigated U_e velocities at [21.07; 26.61; 29.25; 35.48] m/s

A proper masking of the particle images was applied before cross-correlation in order to exclude the strong reflections at the surface of the aluminum model. In Fig. 5 four instantaneous velocity snapshots of all 8 synchronized camera views are shown in the common wall coordinate system for each of the four investigated U_e velocities. The ZPG equilibrium TBL flow can be seen at the two upstream FOV positions and the accelerated FPG-TBL flow in the FOV of positions 3 and 4. Further on, the flow is decelerated in the APG-TBL region as shown in the FOV of position 5 and the overlapping FOV of positions 6, 7 and 8 in downstream order. The flow separates in the APG region earlier for lower flow velocities; intermittency of flow separation is present for all cases over a relatively large area in flow direction.

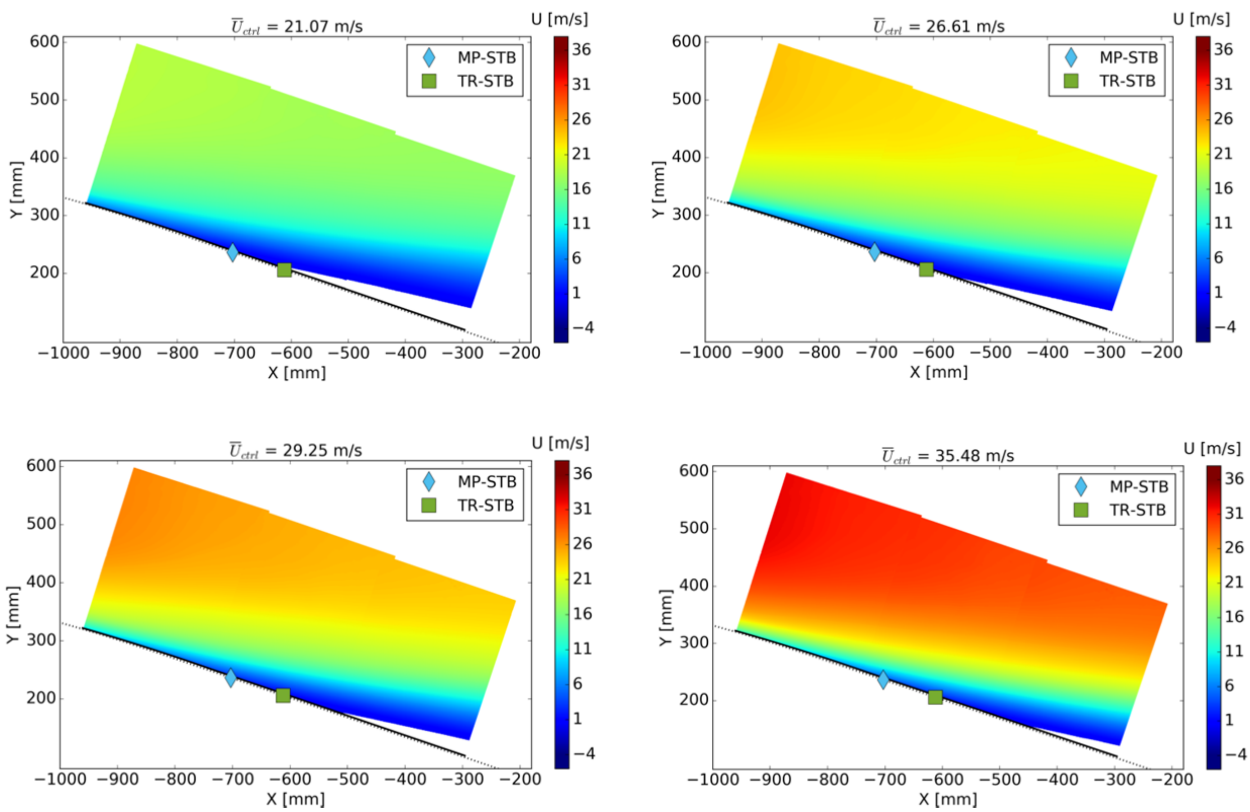

<u>Figure 6:</u> Averaged u-velocity distributions of the TBL flow for the APG region for all four U_e velocities indicating the mean point of flow separation (mean wallparallel reverse flow regions are coded white) and measurement midpoints of the MP-STB and 3D-STB systems are marked with blue diamond and green square markers respectively.

The corresponding average flow fields indicating points of mean separation are displayed in Fig. 6 for all four velocities. Due to the unsteadiness of the flow separation, and to the development of turbulent fluctuations in the shear layer above the separated flow, the corresponding

Reynolds stresses <*u'v'*> are high in the related regions; the maximum is first growing and then broadening along the APG region while moving away from the wall in downstream direction (see Fig. 7). Further downstream of the mean separation point a plateau of high values of <*u'v'*> seem to be reached.

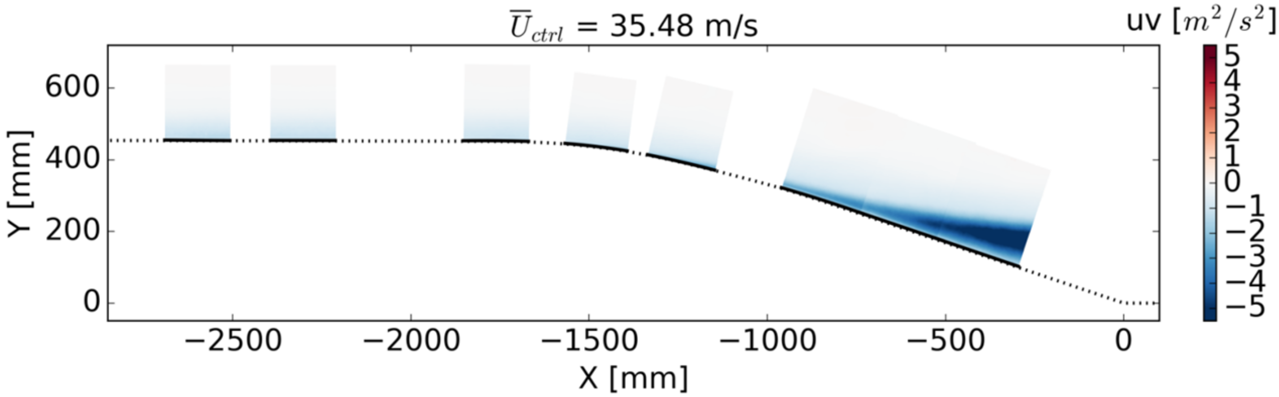

Figure 7: Distribution of Reynolds stress <u'v'> along the TBL flow showing increased and wall-normal broadened values in the APG region; the maximum of turbulence production moves away from the wall along the downstream direction and reaches the highest values above the separated flow region.

A novel 2D Lagrangian particle tracking method (2D-STB) has been recently developed at DLR, based on the 3D-STB code. In the following the performances of the 2D-STB particle tracking method in terms of spatial resolution are compared with the classical cross-correlation approach using non-isotropic window sizes; a direct comparison between the two approaches is possible as they are carried out on the same data-set of time-resolved images gained in the ZPG region (s. Chapter 2 on 2D-STB). The PIV evaluation scheme is described first and is related to Willert (2015). In order to allow for high wall-normal spatial resolution of the velocity vector fields, an iterative window deformation scheme using final window sizes of 48 x 6 pixel^2 in x- and y-direction has been used for the cross-correlation of subsequently acquired particle images. The mean velocity and corresponding Reynolds stress profiles based on the given cross-correlation scheme are shown in Fig. 8 (left and right respectively). First, one can see the remarkable growing of the second peak in the <u'u'> curves compared to the lower Reynolds number DNS solution, which is a well reported physical effect caused by the presence of s.c. superstructures. On the other hand, closer to the wall the resolution is clearly limited and the mean velocity profiles, for both U_e = 29.25 and 35.48 m/s, deviate from the given DNS solution (available at a lower Re_θ of 6500) already around y+ = 30 . Consequently the <u'u'> curves on the right side of Fig. 8 deviate from the DNS already below y+~= 50 and, due to the much smaller structure sizes of the v'-events - especially in flow direction, the <v'v'> curve is underestimated when compared to the corresponding Reynolds stresses given by the DNS solution. This occurs over the major part of the wall-normal measurement area due to the low-pass filter effect of the correlation windows. In conclusion, the adapted cross-correlation method is not applicable anymore close to the wall for such high Reynolds number TBL flows or for such small viscous units of l+ ~13.5 μm respectively (l+ was estimated preliminary from RANS simulations for U_e = 36 m/s at the given measurement position in the ZPG region). With ~ 43 μm/pixel image magnification of the given high-speed camera and lens system one would need a good subpixel resolution in order to reach the required resolutions.

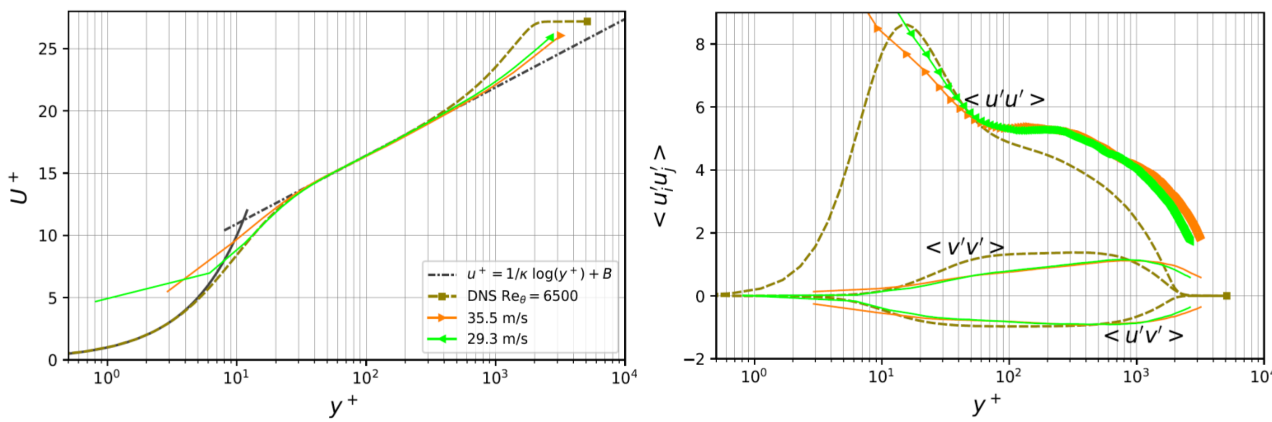

Figure 8: Mean velocity and Reynolds stress profiles based on PIV evaluation with non-isotropic correlation window sizes (48 x 6 px²) in the ZPG region for two U_e velocities and the DNS solution of a lower Reynolds number flow and law-of-the-wall for comparison

Recently, the Shake-The-Box Predictor/Corrector-scheme has been adapted to allow for the tracking of particles on time-resolved recordings based on single camera views (yielding time-resolved 2D2C velocity data along tracks). The new 2D-STB evaluation scheme is based on the core functionality of STB (predicting particle positions, correcting for the introduced error by 'shaking' the predicted particle position (similar to IPR (Wieneke 2013)), however the volume reconstruction is replaced by a simple peak search on the 2D image. The method works reliably in finding tracks in images with moderate particle image densities. A synthetic test based on a ppp (particles per pixel) variation is foreseen. The method is computationally efficient ascales with the number of tracked particles. The newly developed STB evaluation is able to identify and follow more than 2,200 particle tracks per time-step for the given image data set (see Fig. 9). An evaluation based on a fraction of the whole data shows the performance gain resulting in a much higher spatial resolution compared to the non-isotropic cross-correlation approach. A bin-averaging scheme with bin-heights of 0.25 pixels (< l+) in wall normal direction has been used which leads to about 100,000 entries per bin for one of three available runs. The limiting factor for a fully converged statistics of such a time-resolved partcile tracking measurement are the temporal scales or turn-over eddy times of superstructures embedded in the outer logarithmic region of the TBL flow (~0.4 δ).

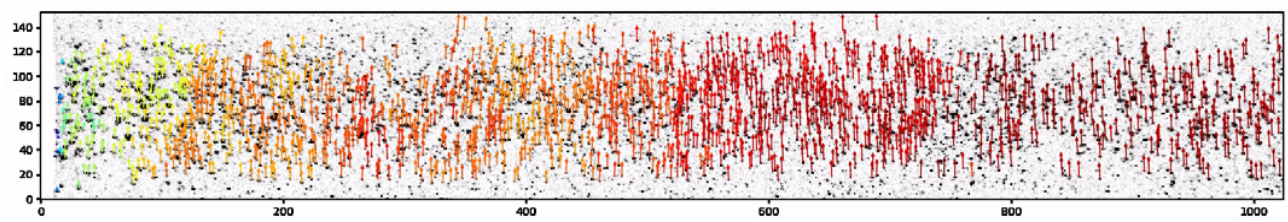

Figure 9: Particle image out of a 50 kHz time series acquired in the ZPG region of the TBL flow and color coded u-velocity vectors at found particle tracks based on the newly developed 2D-STB particle tracking approach.

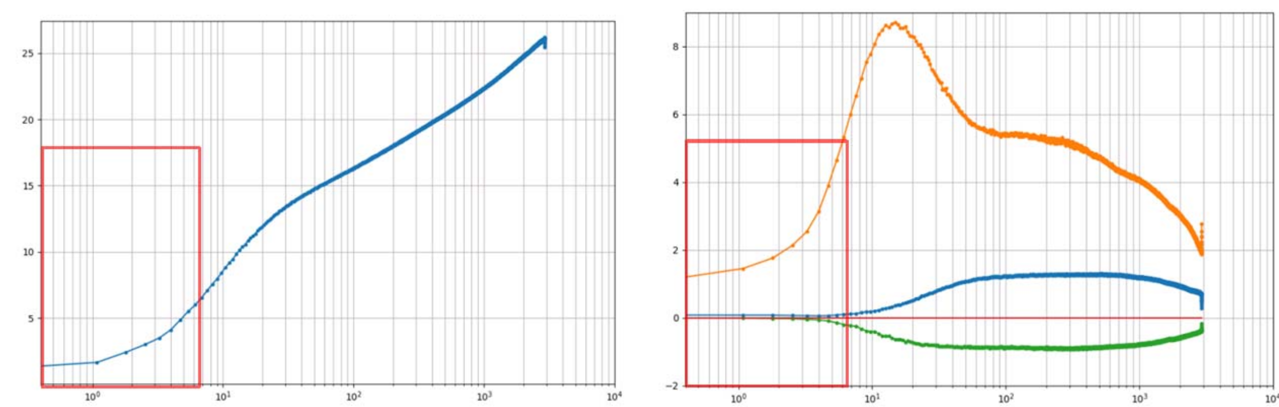

Figure 10: Mean velocity in m/s (left) and Reynolds stress <u’u’>, (v’v’) and <u’v’> profiles in m^2/s^2 (top to bottom right) based on 2D-STB particle tracking in the ZPG region for U_e = 35.5 m/s bin size smaller than l+ ~13.5 μm). Red rectangle marks first two pixels above the wall.

Both the mean and Reynolds stress profiles retain the main features of the ZPG-TBL flow as shown in Fig. 10 left and right. The first peak at y+ = 13 for <u’u’> can be nicely resolved and the <v’v’> and <u’v’> curves are not underestimated anymore along the wall-normal direction, because no low-pass filtering effects are present. In the very near wall area below y+ = 4 to 5, corresponding to ~60 μm (~1.4 pixels), still a deviation from the DNS solution for mean and Reynolds stresses at <u’u’> can be detected. Here a special treatment of overlapping true and mirrored particle images directly at wall need to be found; the use of an adaptive double-peak OTF, couple with a suitable peak-finding strategy, can be forseen in order to further enhance the profile quality close to the wall.

For the 3D-STB evaluation based on the time series of particle images from the four *iSpeed726* cameras, a similar evaluation scheme as described in Schanz et al. 2016 has been applied. The optically distorted particle images require the above mentioned OTF calibration for a proper image matching scheme with the tracking approach.

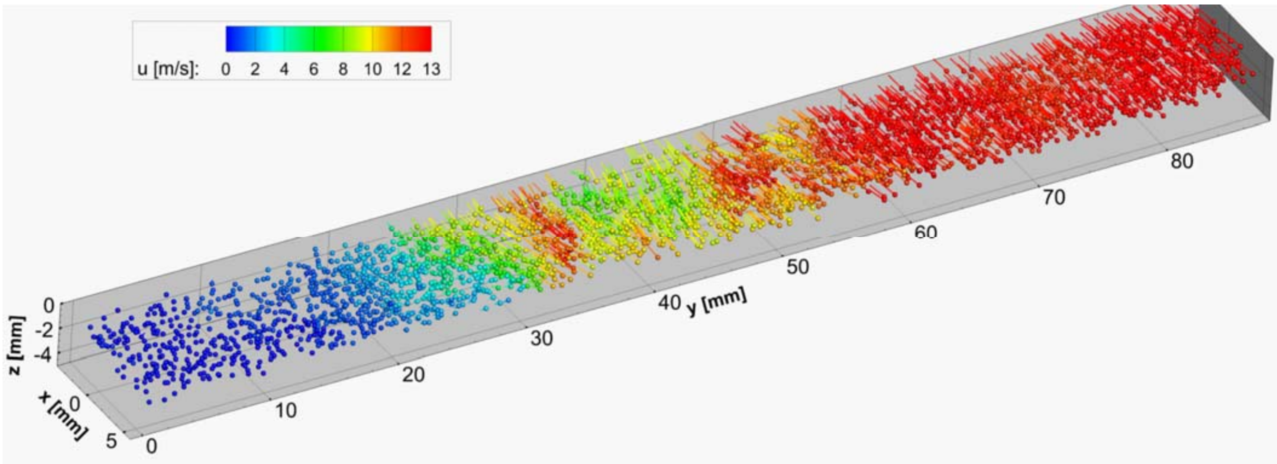

Figure 11: Time resolved 3D-STB tracking result with ~3,000 particles at U_e = 21 m/s in the APG region of the TBL flow (with intermittent flow separation at mean separation position). Wall coordinate system X*, Y*, Z*

Here approximately 3,000 particles per time-step are found and tracked while 2,715 chunks á 109 images have been evaluated per flow case. Additionally, fully time resolved particle image series with up to 25,000 frames have been captured in order to show the temporal behavior of the flow separation over a longer sequence. A volumetric velocity field based on the tracked particles at one time step within the time-resolved series is given in Fig. 11 showing the u-component of velocity color coded. At U_e = 21 m/s, the mean flow-separation point is located within the 3D-STB volume. The snapshot shows particles with zero or slightly negative wall-parallel flow velocities close to the wall (< y ~ 15 mm), while at y = 80 mm the typical outer-layer flow with low velocity fluctuations is present within the same column-shaped wall-normal measurememnt volume. Given the availability of the full 3D3C velocity information along the distributed particle trajectories with position accuracies of ~5 μm per fitted track (accuracy from frequency spectrum of the unfitted particle tracks), a bin-averaging approach has been used for gaining the fluid mechanical relevant flow statistics. Mean and Reynolds stress profiles of all 3-components of velocity for two (of four) U_e velocities at are shown in Fig. 12. With 150,000 to 300,000 entries per single px (~ 40 μm) bin a very good convergence of the mean flow statistics and Reynolds stresses is possible down to the wall. However, the long temporal scales of the intermittent separated flow and the superstructures would need even longer measurement times or more statistically independent entries for a decent higher order flow statistics. In our case the limitation of the download rate of the IX camera and the restriction to chunks of at least 109 images length inhibit such a fully converged statistics. Given the recently optimized fast STB implementation, the evaluation time of such long image series does not represent a bottleneck.

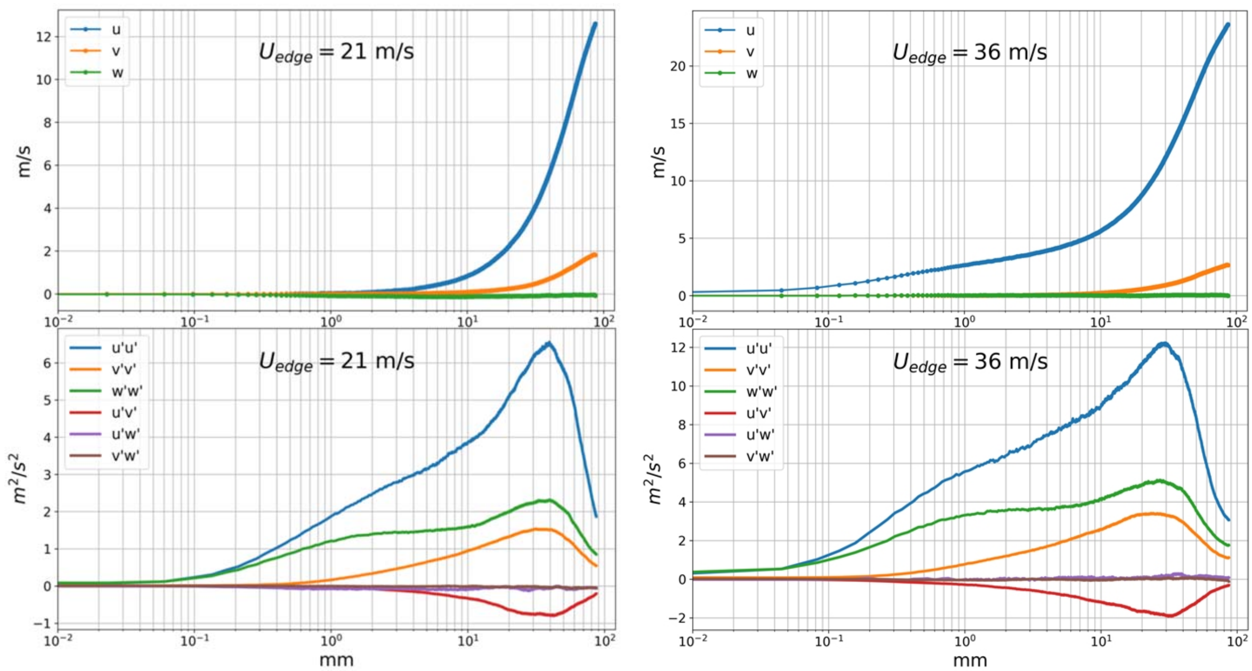

<u>Figure 12:</u> Bin-averaged mean and Renolds stress profiles of all 3-components of velocity from time-resolved 3D-STB measurements in the APG region of the TBL flow. *Left:* At the mean flow separation position at U_e = 21 m/s. *Right:* At U_e = 36 m /s. Wall coordinate system X*, Y*, Z*

In addition to the time-resolved Lagrangian particle tracking techniques presented above, a Multi-Pulse STB investigation has been performed, which allows for the reconstruction of individual particle tracks within a relatively large volume of 80×90×6 mm^3. Short time-resolved sequences of four-pulses have been generated by means of a dual illumination system and images have been recorded by a 3D imaging system consiting in four PCO Edge cameras. Sequences of 40,000 multi-pulse recordings have been acquired at 10 Hz, providing statistically independent 3D3C short-tracks result suitable for the evaluation of highly spatially resolved and statistically converged boundary layer profiles.

A novel approach for the acquisitoin of the four-pulse sequences based on the adoption of multi-exposed recordings (two pulses imaged for each of the camera frames) has been adopted here; a more detailed description of the acquisition strategy can be found in Novara et al. 2018.

The results are very promising and the data-set allows for multiple approaches of statistical analyses due to the relatively large volume and the statistically independent track fields. An instantaneous snapshot of the MP-STB results containing ~20,000 four pulse particle tracks is shown in Fig. 13-left. The directional ambiguities caused by the use of double-exposed images is resolved thanks to the availability of four-pulses as potentially ambigous two-pulse tracks (independently reconstructed for each frame) are univocally combined into four-pulse tracks. This is confirmed by the capabiltiy of the MP-STB algorithm of resolving the significant back-flow events occuring within the measurement volume at low speeds (Fig. 13-left).

An ensemble averaging of the MP-STB results has been carried for the U_e = 35.48 m/s case; scattered results from the tracking method have been collected into 2D bins of approximately 16 × 0.07 mm² (450 × 2 px). The mean velocity components alonng the wall-normal and wall-parallel components are shown in Fig 13-right relative to central location of the FOV along the wall-parallel direction.

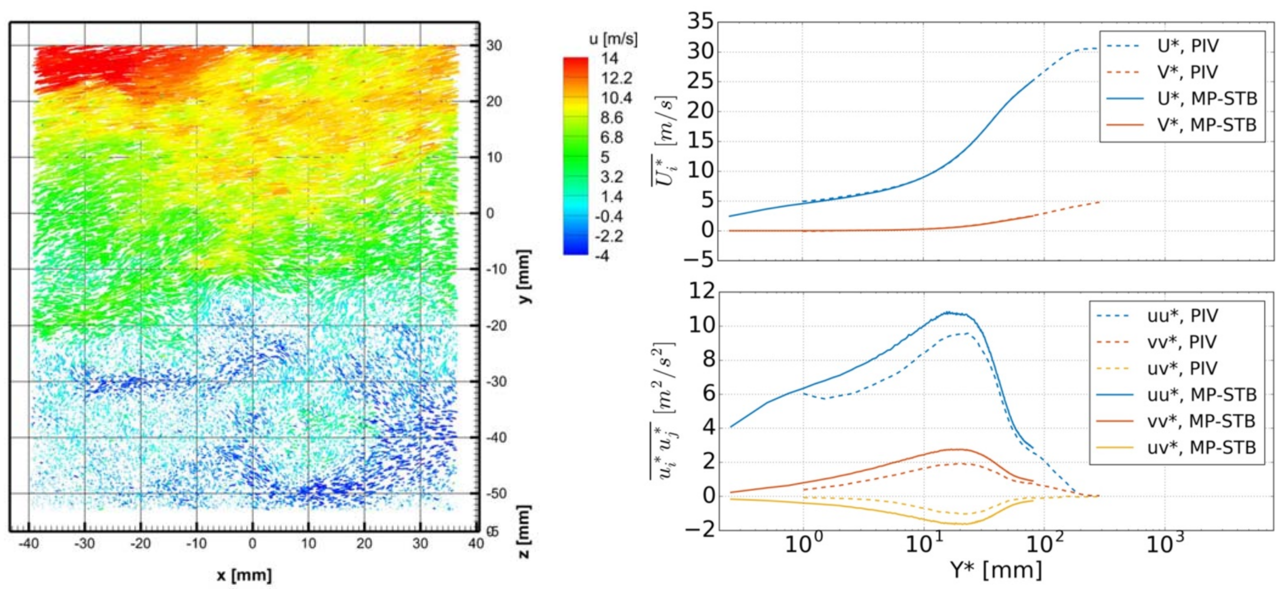

Figure 13: Track results of MP-STB measurements. *Left:* Representation of ~20,000 4-pulse tracks with flow separation for U_e = 21.1 m/s in APG region. *Right:* Bin-averaged mean and Reynolds stress profiles for 2-components of velocity from MP-STB (solid lines)with direct comparison to 2D2C-PIV profiles (dashed lines) showing the low-pass filtering effects of PIV at U_e = 35.5 m/s

Results are directly compared with those from the planar PIV measurment at the same location (dashed lines); a good agreement is found for the mean *u*- and *v*- velocity profiles. On the other hand, when the Reynolds stresses are considered, the modulation of the signal introduced by the finite size of the cross-correlation window is visible for the PIV results. This leads to lower values of the fluctuation intensities for both velocity components. As expected, the results from the MP-STB Lagrangian particle tracking method do not suffer from the same low-pass filtering effect.

4. Conclusions

An experimental investigation of an adverse pressure gradient turbulent boundary layer (TBL) flow at high Reynolds numbers (approx. 10.000 < Re_θ < 40.000) has been succesfully performed in the frame of the DLR project *Victoria* and conducted in the Eiffel type atmospheric wind tunnel of the University of Armed Forces in Munich (AWM). Several particle based optical measurement methods have been applied to the flow covering many flow scales with various techniques and fields-of-view by a) large field multi-camera 2D2C PIV, b) time-resolved 2D-Shake-The-Box (STB) Lagrangian particle tracking at 30 to 50 kHz in the ZPG and FPG flow region, c) time-resolved 3D- STB Lagrangian particle tracking at 20 to 40 kHz in the APG flow region and d) Multi-Pulse (MP-) 3D-STB in the APG flow region. The gained results offer the possiblity to apply global and local statistical flow analysis tools with the goal to enhance the understanding of the APG TBL flow and related dynamics down to (intermittent) flow separation. In a first step high resolution mean flow statistics and related Reynolds stresses have been calculated in order to provide validation data for new scaling laws and turbulence models in advanced RANS simulation methods aiming at an improvement of the prediction capabilities for APG TBL flows with incipient flow separation e.g. for high-lift-wing aerodynamics.

5. References

Gesemann S, Huhn F, Schanz D and Schröder A (2016), From Noisy Particle Tracks to Velocity, Acceleration and Pressure Fields using B-splines and Penalties, 18th Int Symp on the Application of Laser Techniques to Fluid Mechanics, July 4-7, Lisbon, Portugal

Knopp T, Buchmann N A, Schanz D, Eisfeld B, Cierpka C, Hain R, Schröder A. & Kähler C J (2015), Investigation of scaling laws in a turbulent boundary layer flow with adverse pressure gradient using PIV. Journal of Turbulence 16, 250–272.

Knopp T, Schanz D, Schröder A, Dumitra M, Hain R & Kähler C J (2014), Experimental investigation of the log-law for an adverse pressure gradient turbulent boundary layer flow at Re_θ up to 10000. Flow, Turbulence and Combustion 92, 451–471.

Maciel Y, Rossignol K S & Lemay J (2006), Self-Similarity in the Outer Region of Adverse-Pressure-Gradient Turbulent Boundary Layers, AIAAJ 44, 2450–2464.

Manovski P, Depuru Mohan NK, Geisler R, Novara M, Schanz D, Agocs J, Ahlefeldt T, Spehr C and Schröder A (2016), 3D Lagrangian particle tracking using 4-pulse Shake-The-Box synchronized with microphone measurements on a subsonic jet at Mach 0.9, NIOPLEX Workshop, October 25-26, Delft, The Netherlands

Michaelis D, Neal RD, Wieneke B (2016), Peak-locking reduction for particle image velocimetry, Meas. Sci. Technol. 27, 104005

Novara M, Schanz D, Geisler R, Voss C and Schröder A (2017), Pulse separation strategies for multi-pulse systems: 3D Lagrangian particle tracking with Shake-The-Box in turbulent boundary layers, 12th International Symposium on Particle Image Velocimetry, June 19-21, Busan, Korea

Novara M, Schanz D, Reuther N, Kähler CJ and Schröder A (2016), Lagrangian 3D particle tracking in high-speed flows: Shake-The-Box for multi-pulse systems, Exp in Fluids 57:128

Novara M, Schanz D, Geisler R, Voss C and Schröder A (2017), Pulse separation strategies for multi-pulse systems: 3D Lagrangian particle tracking with Shake-The-Box in turbulent boundary layers" 12th International Symposium on Particle Image Velocimetry, June 19-21, Busan, Korea

Novara M, Schanz D, Geisler R, Voss C and Schröder A (2018), Multi-Exposed recordings for 3D Lagrangian particle tracking in turbulent boundary layer flows by means of Multi-Pulse Shake-The-Box, 19th Int Symp on the Application of Laser Techniques to Fluid Mechanics, July 16-19, Lisbon, Portugal

Nickels TB (2004), Inner scaling for wall-bounded flows subject to large pressure gradients. Journal of Fluid Mechanics 521, 217–239.

Raffel M, Willert C, Wereley S, Kompenhans J (2007), Particle image velocimetry: a practical guide, Exp Fluid Mech, Springer, Berlin

Schanz D, Gesemann S, Schröder A, Wieneke B and Novara M (2013), Non-uniform optical transfer function in particle imaging: calibration and application to tomographic reconstruction, Meas Sci Technol 24, 024009

Schanz D, Gesemann S and Schröder A (2016), Shake-The-Box: Lagrangian particle tracking at high particle image densities, Exp In Fluids 57:70

Schneiders JFG, Scarano F (2016) Dense velocity reconstruction from tomographic PTV with material derivatives, Exp In Fluids 57: 139.

Schröder A, Schanz D, Michaelis D, Cierpka C, Scharnowski S and Kähler CJ (2015a), Advances of PIV and 4D-PTV "Shake-The-Box" for Turbulent Flow Analysis – the Flow over Periodic Hills, Flow Turbulence and Combustion), 95 (2-3): 193-209.

Schröder A, Schanz D, Gesemann S, Willert C (2015b), Near-wall turbulence characterization using 4D-PTV Shake-The-Box, 11th International Symposium on Particle Image Velocimetry - PIV2015, 14. - 16. Sept. 2015, Santa Barbara, CA, USA

Wieneke B (2013), Iterative reconstruction of volumetric particle distribution, Meas Sci Technol 24, 024008

Willert C (2015), High-speed particle image velocimetry for the efficient measurement of turbulence statistics. Exp Fluids 56:17